



UNIVERSITÀ
DEGLI STUDI
FIRENZE

FLORE

Repository istituzionale dell'Università degli Studi di Firenze

Determination of 3D Coronal Structures from UVCS/SOHO Synoptic Observations

Questa è la Versione finale referata (Post print/Accepted manuscript) della seguente pubblicazione:

Original Citation:

Determination of 3D Coronal Structures from UVCS/SOHO Synoptic Observations / L. Strachan;A. V. Panasyuk;S. Fineschi;L. D. Gardner;J. C. Raymond;E. ANtonucci;S. Giordano;M. Romoli;G. Noci;J. L. Kohl. - STAMPA. - 415:(1997), pp. 539-+. (Intervento presentato al convegno ESA-SP 415. Correlated Phenomena at the Sun, in the Heliosphere and in Geospace nel 1997-#dec#).

Availability:

This version is available at: 2158/383123 since:

Terms of use:

Open Access

La pubblicazione è resa disponibile sotto le norme e i termini della licenza di deposito, secondo quanto stabilito dalla Policy per l'accesso aperto dell'Università degli Studi di Firenze (<https://www.sba.unifi.it/upload/policy-oa-2016-1.pdf>)

Publisher copyright claim:

(Article begins on next page)

DETERMINATION OF 3D CORONAL STRUCTURES FROM UVCS/SOHO SYNOPTIC OBSERVATIONS

L. Strachan¹, A.V. Panasyuk¹, S. Fineschi¹, L.D. Gardner¹, J.C. Raymond¹,
E. Antonucci², S. Giordano³, M. Romoli⁴, G. Noci⁴, and J.L. Kohl¹

¹ Harvard-Smithsonian Center for Astrophysics, Cambridge, MA 02138, USA

² Osservatorio Astronomico di Torino, I-10025 Pino Torinese, Italy

³ Università di Torino, I-10125 Torino, Italy

⁴ Università di Firenze, I-50125 Firenze, Italy

ABSTRACT

Daily coronal synoptic observations made with the Ultraviolet Coronagraph Spectrometer on SOHO (UVCS/SOHO) are used to create Carrington maps of line-of-sight intensities and spectral line widths for H I Lyman alpha and the O VI 1032/1037 doublet. These 2D maps can then be used as inputs to a tomographic inversion routine to produce 3D models of the corona out to $2.5 R_{\odot}$ in the polar regions ($3.0 R_{\odot}$ in equatorial regions). The initial results for the determination of O^{5+} outflow velocities as a function of heliographic latitude is presented.

Key words: solar corona; solar wind.

1. INTRODUCTION

The Ultraviolet Coronal Spectrometer (UVCS) on SOHO (Kohl et al., 1995) measures the intensity and profile of several EUV emission lines in the solar corona. The brightest and most important is the H I Lyman alpha line at 1216 \AA . The next brightest coronal lines in this part of the spectrum are the O VI doublet lines at 1032 and 1037 \AA . Maps of the intensity and profile of these lines are made daily by scanning the UVCS spectrometer slits completely around the occulted disk of the Sun. As the Sun and corona rotates these two dimensional images give different views of the corona that can be used to reconstruct the three dimensional structure of the corona. The data set used for the observations in this study was obtained during the SOHO Whole Sun Month Campaign (Biesecker et al., 1997). A description of the observations is given in Strachan et al. (1997).

One of the goals of the present study is to obtain true 3D structures based on a reconstruction of the true coronal emissivities. What is normally observed in a single observation are the line of sight integrated intensities. Panasyuk et al. (1997) discuss how the synoptic measurements of coronal intensities can be used

to reconstruct the local emissivities in the corona. Once the local emissivities are determined, the true dimensions of structures along the line of sight can be determined.

In addition to describing the true dimensions of coronal structures, one can also obtain more reliable estimates of coronal outflow velocities based on the Doppler dimming technique (Withbroe et al., 1982; Noci, Kohl, & Withbroe, 1987). For the present study we concentrate on the determination of latitudinal dependence of the O^{5+} outflow velocities based on the Carrington maps constructed from Whole Sun Month observations.

2. SYNOPTIC OBSERVATIONS

Daily synoptic observations were used to create maps of intensities versus latitude and time (longitude) for the O VI doublet lines (Strachan et al., 1997). Figures 1 and 2 show Carrington maps for Rotations 1912 to 1914 for O VI 1032 and 1037. The relative enhancement in emission in the narrow equatorial regions is due to the higher O^{5+} density in the regions of closed magnetic field lines and because of the Doppler dimming of the O VI emission where there are regions of high outflow velocities. There is also an intensity variation within the center streamer belt that is thought to be due to a relative depletion in the O^{5+} abundance (Raymond et al. 1977).

The scale used in Figures 1 and 2 is a relative scale where the intensities are highest (lowest) for the lighter (darker) shadings. The black or white streaks are places where there are defects in the data. The color table for the maps at $2.25 R_{\odot}$ had to be pushed to show the fainter features. Data for almost 2.5 solar rotations are shown.

These maps do not show the intensity distributions of real structures since they show line of sight intensities which are integrated over a long path length through the optically thin corona. However, because points near the plane of the sky are also closer to the disk, the line of sight tends to pick out the fea-

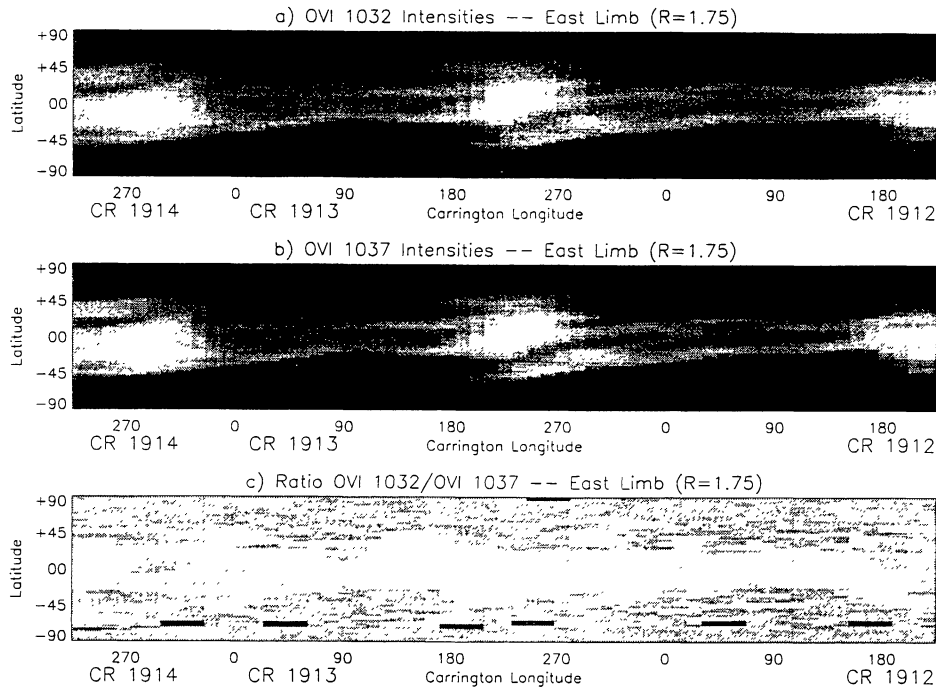


Figure 1. Carrington maps for $r = 1.75 R_{\odot}$ of a) O VI 1032 intensities, b) O VI 1037 intensities, and c) Ratio of intensities 1032/1037. See text for explanation.

tures near the plane of the sky. Localized features tend to be stretched out in longitude, but these can be reconstructed by proper tomographic techniques (Panasyuk et al., 1997).

It is interesting to compare these maps with those of Wang et al. (1997) which show the distribution of emission from Thomson scattered visible light. The authors modeled the streamer belt with a simple dipole magnetic field and a current sheet near the equatorial equator. The streamer structures as seen in the Carrington maps form a narrow belt around the current sheet. The O VI emission show similar features including the opposite tilts of high latitude structures seen when comparing East and West limb Carrington maps for the same Carrington rotation. Wang et al. (1997) explain this tilt as an effect caused by the 7 degree tilt in the solar rotation axis.

3. DETERMINATION OF O^{5+} OUTFLOW VELOCITIES

When a model of the observed coronal regions is made using inputs from white light coronagraphs (to get electron density) and *in situ* measurements (to constrain electron temperature) as well as the UVCS spectroscopic measurements (intensities and profiles) then a map of the outflow velocities can be made from

the UVCS O VI intensity ratios.

The intensity ratios, $I(1032)/I(1037)$, are shown in Panel (c) of Figures 1 & 2. Note that the contrast between the streamer belt and polar coronal holes is greater at the higher heliocentric height. This is because the acceleration of the wind from 1.75 to $2.25 R_{\odot}$ is larger in the coronal hole regions than in the streamer belt. The larger acceleration is such that the coronal hole intensities are Doppler dimmed much faster away at $2.25 R_{\odot}$. (There is a density effect as well but this can be factored out using the densities derived from white light data.)

The UVCS OVI intensity synoptic maps can be used to estimate outflow velocities of O^{5+} by taking ratios for the O VI 1032 and 1037 intensities (Noci, Kohl, & Withbroe, 1987). These are estimates since the synoptic maps at the present show line of sight integrated intensities. Panasyuk et al. (1997) have developed a method of reconstructing the actual emissivities for the coronal lines and these can be used to obtain more accurate outflow velocities. For this work we use the fact that the configuration of the corona near solar minimum has a high degree of symmetry about the solar rotation axis during a large fraction of each solar rotation.

We exploit the symmetry in order to take averages over appropriate longitude ranges where the coronal configuration consists of a single equatorial streamer

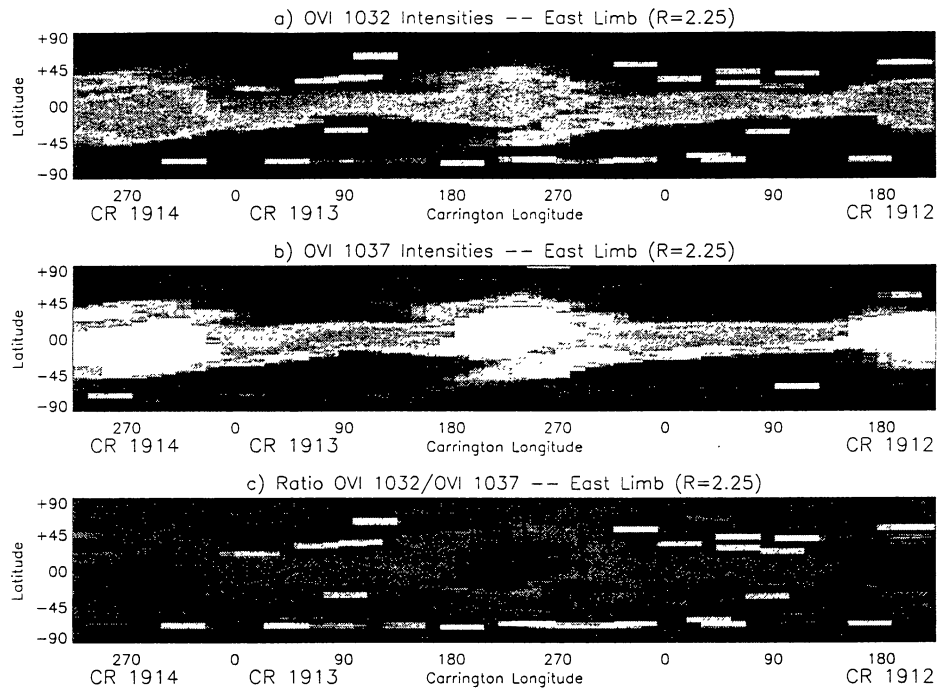


Figure 2. Carrington maps for $r = 2.25 R_{\odot}$ of a) O VI 1032 intensities, b) O VI 1037 intensities, and c) Ratio of intensities 1032/1037. Note that the color table was adjusted to show the fainter features at this height in the corona. See text for explanation.

belt and two large polar coronal holes. This configuration occurred during 15 – 21 Aug. 1996 on the West limb (Carrington Longitudes 93° to 176°).

Outflow velocities were computed by averaging the observed intensities at 80 position angles from the north to south heliographic pole for the O VI lines at $1.75 R_{\odot}$ and $2.25 R_{\odot}$. The averages were made taking the mean intensity from 7 daily synoptic observations (approximately $1/4$ of a solar rotation). This data set was chosen since it includes a stable streamer arcade which is a main target of study for the SOHO Whole Sun Month data analysis.

The goal is to compute the O^{5+} outflow velocities as a function of latitude. To do this one must use a model of the corona which can predict the observed line ratios using the outflow velocity as a free parameter. The model uses constraints for the coronal plasma parameters (densities and kinetic temperatures for the electrons, protons and ions). Similar to the treatment by Kohl et al. (1997); Cranmer et al. (1997), we use freezing in temperatures from Ko et al. (1997) for the assumed electron temperature as a function of height. We use the same electron temperature (as a function of height) for the streamer and coronal hole regions even though, strictly speaking, the temperature profile was determined for a coronal hole. The observed O VI line profiles provide infor-

mation on the microscopic motions of the O^{5+} ions in the direction along the line of sight but not in the direction transverse to the line of sight. Because we lack this information, we assume that the motions of the O^{5+} ions in the radial direction are such that they have the same kinetic temperature (as a function of height) as the electrons.

Kohl et al. (1997) show through an analysis of the O VI line ratios that the microscopic velocity distribution in the radial direction cannot have widths which are much larger than the values assumed for ion-electron equilibrium (especially for the higher heights). In any case, by using the lower limit on the velocity distribution widths in the radial direction, a lower limit on the outflow velocity is determined from Doppler dimming. If it is assumed that the O^{5+} velocity distribution in the radial direction were wider then even larger outflow speeds would be expected.

The electron densities for the coronal holes and streamer belt are based on an analysis of white light polarized brightness data from Mauna Loa observations made during the same period of time as the UVCS/SOHO observations (Gibson, 1997). The densities are assumed to be constant throughout the coronal holes and the streamer belt, although different density models were used for the two regions.

4. RESULTS

Figure 3 shows the outflow velocity for O^{5+} as a func-

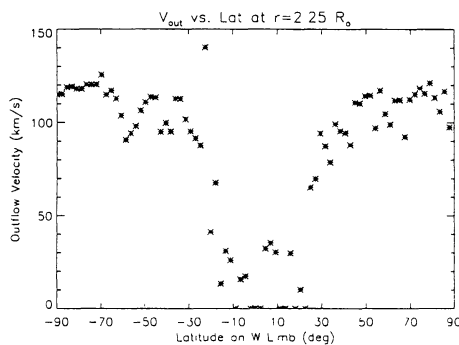


Figure 3. Outflow velocity vs. latitude at $2.25 R_{\odot}$ for a coronal streamer surrounded by two polar coronal holes. The coronal region was centered on the West limb on 18 Aug 1996.

tion of latitude at $2.25 R_{\odot}$. The data points at zero correspond to places where the values for the outflow velocity were indeterminate (but not necessarily zero). The data are averaged over eight days centered on 18 Aug. 1996 on the West limb. The scatter in the data gives idea of the relative uncertainty in the outflow velocity determinations. The uncertainty in the velocity at in each point can be as large a factor of two if one assumes that the width of the microscopic velocity distribution in the radial direction is comparable to the width of the observed $O VI$ line profiles. As mentioned above, this case is probably unlikely and the uncertainties are should be somewhat smaller. These velocity results can be improved when treated in a self-consistent manner as was done by Kohl et al. (1997) for the axis of coronal hole.

5. CONCLUSIONS

This paper presents the first results on the longitudinal dependence of O^{5+} outflow velocities based on UVCS synoptic observations of the $O VI$ doublet line ratios. Improvements can be made by using a self-consistent model that incorporates the true emissivities rather than the line of sight intensities that have been used here. A self-consistent coronal model can be used to provide constraints on possible differences in the solar wind acceleration in coronal streamers versus polar coronal holes.

ACKNOWLEDGMENTS

This work is supported by NASA under Grant NAG5-3192 to the Smithsonian Astrophysical Observatory, by the Italian Space Agency, and by Swiss funding sources.

REFERENCES

- Biesecker, D., Alexander, D., Altrrock, R.C., DeForest, C., Fludra, A., Forsyth, B., Galvin, T., Gibson, S., Hassler, D., Henry, T.W., Hoeksema, J.T., Korendyke, C., Lazurus, A., Lecinski, A., Leping, R., Panasyuk, A., Riley, P., Steinberg, J., Strachan, L., Thompson, B., Summanen, T., & Szabo, A. 1997, Proc. Fifth SOHO Workshop, (in press)
- Cranmer, S.R., Field, G.B., Noci, G., & Kohl, J.L., 1997, these proceedings
- Gibson, S.E. 1997, Personal Communication
- Ko, Y.-K., Fisk, L.A., Geiss, J., Gloeckler, G. & Guhathakurta, M. 1997, Solar Phys. 171, 345
- Kohl, J.L., Esser, R., Gardner, L.D., Habbal, S., Daigneau, P.S., Dennis, E.F., Nystrom, G.U., Panasyuk, A., Raymond, J.C., Smith, P.L., Strachan, L., van Ballegooijen, A.A., Noci, G., Fineschi, S., Romoli, M., Ciaravella, A., Modigliani, A., Huber, M.C.E., Antonucci, E., Benna, C., Giordano, S., Tondello, G., Nicolosi, P., Naletto, G., Pernechele, C., Spadaro, D., Poletto, G., Livi, S., von der Luhe, O., Geiss, J., Timothy, J.G., Gloeckler, G., Allegra, A., Basil, G., Brusa, R., Wood, B., Siegmund, O.H.W., Fowler, W., Fisher, R., & Jhabvala, M. 1995, Sol. Phys. 162, 313
- Kohl, J.L., Noci, G., Antonucci, E., Tondello, G., Huber, M.C.E., Cranmer, S.R., Strachan, L., Panasyuk, A.V., Gardner, L.D., Romoli, M., Fineschi, S., Dobrzycka, Raymond, J.C., Nicolosi, P., Siegmund, O.H.W., Spadaro, D., Benna, C., Ciaravella, A., Giordano, S., Habbal, S.R., Karovska, M., Li, X., Martin, R., Michels, J., Modigliani, A., Naletto, G., O'Neal, R.H., Pernechele, C., Poletto, G. and Smith, P.L., & Suleiman, R., ApJ Lett. (submitted)
- Noci, G., Kohl, J.L., & Withbroe, G.L. 1987, ApJ 315, 706
- Panasyuk, A.V., Strachan, L., Fineschi, S., Gardner, L.D., Raymond, J.C., Kohl, J.L., Antonucci, E., Giordano, S., & Romoli, M. 1997, Proc. 18th NSO/SP Summer Workshop, (in press)
- Raymond, J.C., Kohl, J.L., Noci, G., Antonucci, E., Tondello, G., Huber, M.C.E., Gardner, L.D., Nicolosi, P., Fineschi, S., Romoli, M., Spadaro, D., Siegmund, O.H.W., Benna, C., Ciaravella, A., Cranmer, S., Giordano, S., Karovska, M., Martin, R., Michels, J., Modigliani, A., Naletto, G., Panasyuk, A., Pernechele, C., Poletto, G., Smith, P.L., Suleiman, R.M., & Strachan, L. 1997, Sol. Phys., in press
- Strachan, L., Raymond, J.C., Panasyuk, A.V., Fineschi, S., Gardner, L.D., Antonucci, E., Giordano, S., Romoli, M., Noci, G., & Kohl, J.L. 1997, Proc. Fifth SOHO Workshop, (in press)
- Wang, Y.-M., Sheeley, N.R., Jr., Howard, R.A., Kraemer, J.R., Rich, N.B., Andrews, M.D., Brueckner, G.E., Dere, K.P., Koomen, M.J., Korendyke, C.M., Michels, D.J., Moses, J.D., Paswaters, S.E., Socker, D.G., & Wang, D. 1997, ApJ 485, 875
- Withbroe, G.L., Kohl, J.L., Weiser, H., & Munro, R.H. 1982, Space Sci. Rev. 33, 17